Comparison of Photovoltaic Array Maximum Power Point Tracking Techniques

Trishan Esram, *Student Member, IEEE*, and Patrick L. Chapman, *Senior Member, IEEE*

Abstract—The many different techniques for maximum power point tracking of photovoltaic (PV) arrays are discussed. The techniques are taken from the literature dating back to the earliest methods. It is shown that at least 19 distinct methods have been introduced in the literature, with many variations on implementation. This paper should serve as a convenient reference for future work in PV power generation.

Index Terms—Maximum power point tracking (MPPT), photovoltaic (PV).

I. INTRODUCTION

TRACKING the maximum power point (MPP) of a photovoltaic (PV) array is usually an essential part of a PV system. As such, many MPP tracking (MPPT) methods have been developed and implemented. The methods vary in complexity, sensors required, convergence speed, cost, range of effectiveness, implementation hardware, popularity, and in other respects. They range from the almost obvious (but not necessarily ineffective) to the most creative (not necessarily most effective). In fact, so many methods have been developed that it has become difficult to adequately determine which method, newly proposed or existing, is most appropriate for a given PV system.

Given the large number of methods for MPPT, a survey of the methods would be very beneficial to researchers and practitioners in PV systems. Fig. 1 shows the total number of MPPT papers from our bibliography per year since the earliest MPPT paper we found. The number of papers per year has grown considerably of the last decades and remains strong. However, recent papers have generally had shorter, more cursory literature reviews that largely summarize or repeat the literature reviews of previous work. This approach tends to repeat what seems to be conventional wisdom that there are only a handful of MPPT techniques, when in fact there are many. This is due to the sheer volume of MPPT literature to review, conflicting with the need for brevity.

This survey is a single reference of the great majority of papers and techniques presented on MPPT. We compiled over 90 papers pertaining to different MPPT methods published up to the date of submission of this manuscript. It is not our intention to establish a literal chronology of when various techniques were proposed, since the publication date is not necessarily indicative of when a method was actually conceived. As is typical of review papers,
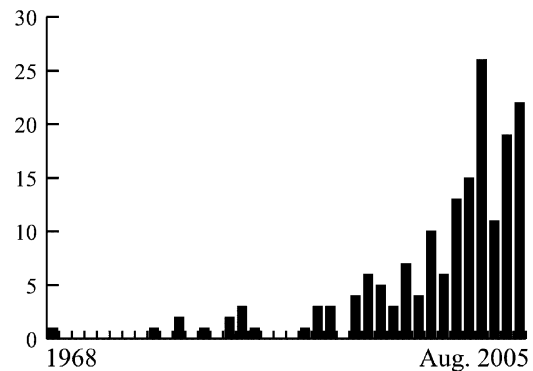
Fig. 1.   Total number of MPPT papers per year, since 1968.

we have elected not to reference patents. Papers referencing MPPT methods from previous papers without any modification or improvement have also been omitted. It is possible that one or more papers were unintentionally omitted. We apologize if an important method or improvement was left out.

This manuscript steps through a wide variety of methods with a brief discussion and categorization of each. We have avoided discussing slight modifications of existing methods as distinct methods. For example, a method may have been first presented in context of a boost converter, but later on shown with a boost-buck converter, otherwise with minimal change. The manuscript concludes with a discussion on the different methods based on their implementation, the sensors required, their ability to detect multiple local maxima, their costs, and applications they suit. A table that summarizes the major characteristics of the methods is also provided.

II. PROBLEM OVERVIEW

Fig. 2 shows the characteristic power curve for a PV array. The problem considered by MPPT techniques is to automatically find the voltage V_{MPP} or current I_{MPP} at which a PV array should operate to obtain the maximum power output P_{MPP} under a given temperature and irradiance. It is noted that under partial shading conditions, in some cases it is possible to have multiple local maxima, but overall there is still only one true MPP. Most techniques respond to changes in both irradiance and temperature, but some are specifically more useful if temperature is approximately constant. Most techniques would automatically respond to changes in the array due to aging, though some are open-loop and would require periodic fine-tuning. In our context, the array will typically be connected to a power converter that can vary the current coming from the PV array.
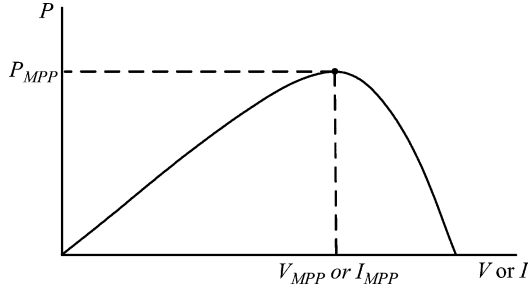
Fig. 2.   Characteristic PV array power curve.

TABLE I
SUMMARY OF HILL CLIMBING AND P&O ALGORITHM

Perturbation	Change in Power	Next Perturbation
Positive	Positive	Positive
Positive	Negative	Negative
Negative	Positive	Negative
Negative	Negative	Positive

III. MPPT TECHNIQUES

We introduce the different MPPT techniques below in an arbitrary order.

A. Hill Climbing/P&O

Among all the papers we gathered, much focus has been on hill climbing [1]–[8], and perturb and observe (P&O) [9]–[25] methods. Hill climbing involves a perturbation in the duty ratio of the power converter, and P&O a perturbation in the operating voltage of the PV array. In the case of a PV array connected to a power converter, perturbing the duty ratio of power converter perturbs the PV array current and consequently perturbs the PV array voltage. Hill climbing and P&O methods are different ways to envision the same fundamental method.

From Fig. 2, it can be seen that incrementing (decrementing) the voltage increases (decreases) the power when operating on the left of the MPP and decreases (increases) the power when on the right of the MPP. Therefore, if there is an increase in power, the subsequent perturbation should be kept the same to reach the MPP and if there is a decrease in power, the perturbation should be reversed. This algorithm is summarized in Table I. In [24], it is shown that the algorithm also works when instantaneous (instead of average) PV array voltage and current are used, as long as sampling occurs only once in each switching cycle.

The process is repeated periodically until the MPP is reached. The system then oscillates about the MPP. The oscillation can be minimized by reducing the perturbation step size. However, a smaller perturbation size slows down the MPPT. A solution to this conflicting situation is to have a variable perturbation size that gets smaller towards the MPP as shown in [8], [12], [15], and [22]. In [24], fuzzy logic control is used to optimize the magnitude of the next perturbation. In [20], a two-stage algorithm is proposed that offers faster tracking in the first stage
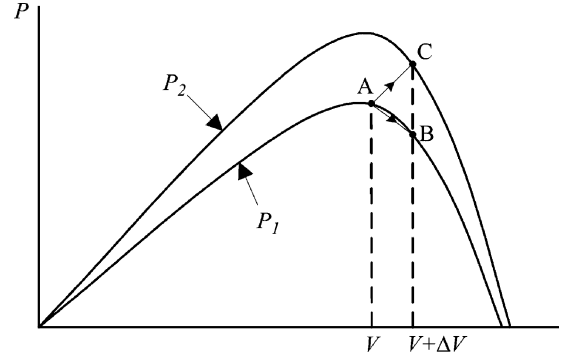

Fig. 3.   Divergence of hill climbing/P&O from MPP as shown in [9].

and finer tracking in the second stage. On the other hand, [21] bypasses the first stage by using a nonlinear equation to estimate an initial operating point close to the MPP.

Hill climbing and P&O methods can fail under rapidly changing atmospheric conditions as illustrated in Fig. 3. Starting from an operating point A, if atmospheric conditions stay approximately constant, a perturbation ΔV in the PV voltage V will bring the operating point to B and the perturbation will be reversed due to a decrease in power. However, if the irradiance increases and shifts the power curve from P_1 to P_2 within one sampling period, the operating point will move from A to C. This represents an increase in power and the perturbation is kept the same. Consequently, the operating point diverges from the MPP and will keep diverging if the irradiance steadily increases. To ensure that the MPP is tracked even under sudden changes in irradiance, [18] uses a three-point weight comparison P&O method that compares the actual power point to two preceding ones before a decision is made about the perturbation sign. In [22], the sampling rate is optimized, while in [24], simply a high sampling rate is used. In [8], toggling has been done between the traditional hill climbing algorithm and a modified adaptive hill climbing mechanism to prevent deviation from the MPP.

Two sensors are usually required to measure the PV array voltage and current from which power is computed, but depending on the power converter topology, only a voltage sensor might be needed as in [7] and [23]. In [25], the PV array current from the PV array voltage is estimated, eliminating the need for a current sensor. DSP or microcomputer control is more suitable for hill climbing and P&O even though discrete analog and digital circuitry can be used as in [4].

B. Incremental Conductance

The incremental conductance (IncCond) [9], [26]–[36] method is based on the fact that the slope of the PV array power curve (Fig. 2) is zero at the MPP, positive on the left of the MPP, and negative on the right, as given by

$$\begin{cases} dP/dV = 0, & \text{at MPP} \\ dP/dV > 0, & \text{left of MPP} \\ dP/dV < 0, & \text{right of MPP.} \end{cases} \quad (1)$$
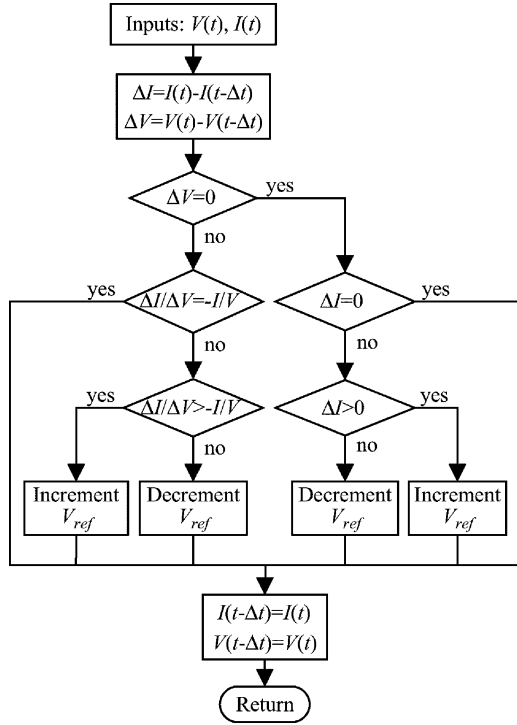
Fig. 4. IncCond algorithm as shown in [29], [32], [33], and [36].

Since

$$\frac{dP}{dV} = \frac{d(IV)}{dV} = I + V\frac{dI}{dV} \cong I + V\frac{\Delta I}{\Delta V} \quad (2)$$

(1) can be rewritten as

$$\begin{cases} \Delta I/\Delta V = -I/V, & \text{at MPP} \\ \Delta I/\Delta V > -I/V, & \text{left of MPP} \\ \Delta I/\Delta V < -I/V, & \text{right of MPP}. \end{cases} \quad (3)$$

The MPP can thus be tracked by comparing the instantaneous conductance (I/V) to the incremental conductance $(\Delta I/\Delta V)$ as shown in the flowchart in Fig. 4. V_{ref} is the reference voltage at which the PV array is forced to operate. At the MPP, V_{ref} equals to V_{MPP}. Once the MPP is reached, the operation of the PV array is maintained at this point unless a change in ΔI is noted, indicating a change in atmospheric conditions and the MPP. The algorithm decrements or increments V_{ref} to track the new MPP.

The increment size determines how fast the MPP is tracked. Fast tracking can be achieved with bigger increments but the system might not operate exactly at the MPP and oscillate about it instead; so there is a tradeoff. In [31] and [35], a method is proposed that brings the operating point of the PV array close to the MPP in a first stage and then uses IncCond to exactly track the MPP in a second stage. By proper control of the power converter, the initial operating point is set to match a load resistance proportional to the ratio of the open-circuit voltage (V_{OC}) to the short-circuit current (I_{SC}) of the PV array. This two-stage alternative also ensures that the real MPP is tracked in case of multiple local maxima. In [37], a linear function is used to divide the I–V plane into two areas, one containing all the possible MPPs under changing atmospheric conditions. The operating point is brought into this area and then IncCond is used to reach the MPP.

A less obvious, but effective way of performing the IncCond technique is to use the instantaneous conductance and the incremental conductance to generate an error signal

$$e = \frac{I}{V} + \frac{dI}{dV} \quad (4)$$

as suggested in [27] and [28]. From (1), we know that e goes to zero at the MPP. A simple proportional integral (PI) control can then be used to drive e to zero.

Measurements of the instantaneous PV array voltage and current require two sensors. IncCond method lends itself well to DSP and microcontroller control, which can easily keep track of previous values of voltage and current and make all the decisions as per Fig. 4.

C. Fractional Open-Circuit Voltage

The near linear relationship between V_{MPP} and V_{OC} of the PV array, under varying irradiance and temperature levels, has given rise to the fractional V_{OC} method [38]–[45].

$$V_{MPP} \approx k_1 V_{OC} \quad (5)$$

where k_1 is a constant of proportionality. Since k_1 is dependent on the characteristics of the PV array being used, it usually has to be computed beforehand by empirically determining V_{MPP} and V_{OC} for the specific PV array at different irradiance and temperature levels. The factor k_1 has been reported to be between 0.71 and 0.78.

Once k_1 is known, V_{MPP} can be computed using (5) with V_{OC} measured periodically by momentarily shutting down the power converter. However, this incurs some disadvantages, including temporary loss of power. To prevent this, [40] uses pilot cells from which V_{OC} can be obtained. These pilot cells must be carefully chosen to closely represent the characteristics of the PV array. In [44], it is claimed that the voltage generated by pn-junction diodes is approximately 75% of V_{OC}. This eliminates the need for measuring V_{OC} and computing V_{MPP}. Once V_{MPP} has been approximated, a closed-loop control on the array power converter can be used to asymptotically reach this desired voltage.

Since (5) is only an approximation, the PV array technically never operates at the MPP. Depending on the application of the PV system, this can sometimes be adequate. Even if fractional V_{OC} is not a true MPPT technique, it is very easy and cheap to implement as it does not necessarily require DSP or microcontroller control. However, [45] points out that k_1 is no more valid in the presence of partial shading (which causes multiple local maxima) of the PV array and proposes sweeping the PV array voltage to update k_1. This obviously adds to the implementation complexity and incurs more power loss.

D. Fractional Short-Circuit Current

Fractional I_{SC} results from the fact that, under varying atmospheric conditions, I_{MPP} is approximately linearly related to the
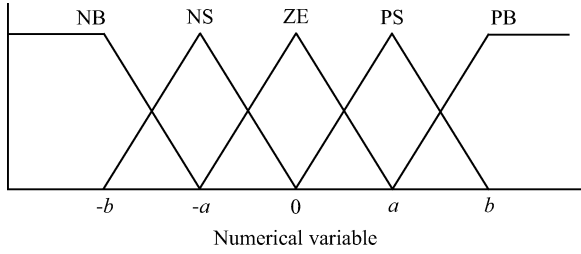
Fig. 5. Membership function for inputs and output of fuzzy logic controller.

TABLE II
FUZZY RULE BASE TABLE AS SHOWN IN [50]

E \ ΔE	NB	NS	ZE	PS	PB
NB	ZE	ZE	NB	NB	NB
NS	ZE	ZE	NS	NS	NS
ZE	NS	ZE	ZE	ZE	PS
PS	PS	PS	PS	ZE	ZE
PB	PB	PB	PB	ZE	ZE

I_{SC} of the PV array as shown in [40], [42], and [45]–[48]

$$I_{MPP} \approx k_2 I_{SC} \qquad (6)$$

where k_2 is a proportionality constant. Just like in the fractional V_{OC} technique, k_2 has to be determined according to the PV array in use. The constant k_2 is generally found to be between 0.78 and 0.92.

Measuring I_{SC} during operation is problematic. An additional switch usually has to be added to the power converter to periodically short the PV array so that I_{SC} can be measured using a current sensor. This increases the number of components and cost. In [48], a boost converter is used, where the switch in the converter itself can be used to short the PV array.

Power output is not only reduced when finding I_{SC} but also because the MPP is never perfectly matched as suggested by (6). In [46], a way of compensating k_2 is proposed such that the MPP is better tracked while atmospheric conditions change. To guarantee proper MPPT in the presence of multiple local maxima, [45] periodically sweeps the PV array voltage from open-circuit to short-circuit to update k_2. Most of the PV systems using fractional I_{SC} in the literature use a DSP. In [48], a simple current feedback control loop is used instead.

E. Fuzzy Logic Control

Microcontrollers have made using fuzzy logic control [49]–[58] popular for MPPT over the last decade. As mentioned in [57], fuzzy logic controllers have the advantages of working with imprecise inputs, not needing an accurate mathematical model, and handling nonlinearity.

Fuzzy logic control generally consists of three stages: fuzzification, rule base table lookup, and defuzzification. During fuzzification, numerical input variables are converted into linguistic variables based on a membership function similar to Fig. 5. In this case, five fuzzy levels are used: NB (negative big), NS (negative small), ZE (zero), PS (positive small), and PB (positive big). In [54] and [55], seven fuzzy levels are used, probably for more accuracy. In Fig. 5, a and b are based on the range of values of the numerical variable. The membership function is sometimes made less symmetric to give more importance to specific fuzzy levels as in [49], [53], [57], and [58].

The inputs to a MPPT fuzzy logic controller are usually an error E and a change in error ΔE. The user has the flexibility of choosing how to compute E and ΔE. Since dP/dV vanishes

at the MPP, [58] uses the approximation

$$E(n) = \frac{P(n) - P(n-1)}{V(n) - V(n-1)} \qquad (7)$$

and

$$\Delta E(n) = E(n) - E(n-1). \qquad (8)$$

Equivalently, (4) is very often used. Once E and ΔE are calculated and converted to the linguistic variables, the fuzzy logic controller output, which is typically a change in duty ratio ΔD of the power converter, can be looked up in a rule base table such as Table II [50].

The linguistic variables assigned to ΔD for the different combinations of E and ΔE are based on the power converter being used and also on the knowledge of the user. Table II is based on a boost converter. If, for example, the operating point is far to the left of the MPP (Fig. 2), that is E is PB, and ΔE is ZE, then we want to largely increase the duty ratio, that is ΔD should be PB to reach the MPP.

In the defuzzification stage, the fuzzy logic controller output is converted from a linguistic variable to a numerical variable still using a membership function as in Fig. 5. This provides an analog signal that will control the power converter to the MPP.

MPPT fuzzy logic controllers have been shown to perform well under varying atmospheric conditions. However, their effectiveness depends a lot on the knowledge of the user or control engineer in choosing the right error computation and coming up with the rule base table. In [55], an adaptive fuzzy logic control is proposed that constantly tunes the membership functions and the rule base table so that optimum performance is achieved. Experimental results from [51] show fast convergence to the MPP and minimal fluctuation about it. In [57], two different membership functions are empirically used to show that the tracking performance depends on the type membership functions considered.

F. Neural Network

Along with fuzzy logic controllers came another technique of implementing MPPT—neural networks [59]–[63], which are also well adapted for microcontrollers.

Neural networks commonly have three layers: input, hidden, and output layers as shown in Fig. 6. The number of nodes in each layer vary and are user-dependent. The input variables can be PV array parameters like V_{OC} and I_{SC}, atmospheric data like irradiance and temperature, or any combination of these. The output is usually one or several reference signal(s) like a
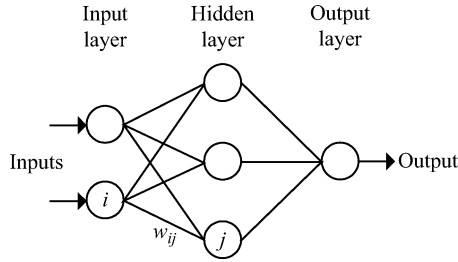
Fig. 6. Example of neural network.

duty cycle signal used to drive the power converter to operate at or close to the MPP.

How close the operating point gets to the MPP depends on the algorithms used by the hidden layer and how well the neural network has been trained. The links between the nodes are all weighted. The link between nodes i and j is labeled as having a weight of w_{ij} in Fig. 6. To accurately identify the MPP, the w_{ij}'s have to be carefully determined through a training process, whereby the PV array is tested over months or years and the patterns between the input(s) and output(s) of the neural network are recorded.

Since most PV arrays have different characteristics, a neural network has to be specifically trained for the PV array with which it will be used. The characteristics of a PV array also change with time, implying that the neural network has to be periodically trained to guarantee accurate MPPT.

G. RCC

When a PV array is connected to a power converter, the switching action of the power converter imposes voltage and current ripple on the PV array. As a consequence, the PV array power is also subject to ripple. Ripple correlation control (RCC) [64] makes use of ripple to perform MPPT. RCC correlates the time derivative of the time-varying PV array power $\dot{p}$ with the time derivative of the time-varying PV array current $\dot{i}$ or voltage $\dot{v}$ to drive the power gradient to zero, thus reaching the MPP.

Referring to Fig. 2, if v or i is increasing ($\dot{v} > 0$ or $\dot{i} > 0$) and p is increasing ($\dot{p} > 0$), then the operating point is below the MPP ($V < V_{MPP}$ or $I < I_{MPP}$). On the other hand, if v or i is increasing and p is decreasing ($\dot{p} < 0$), then the operating point is above the MPP ($V > V_{MPP}$ or $I > I_{MPP}$). Combining these observations, we see that $\dot{p}\dot{v}$ or $\dot{p}\dot{i}$ are positive to the left of the MPP, negative to right of the MPP, and zero at the MPP.

When the power converter is a boost converter as in [64], increasing the duty ratio increases the inductor current, which is the same as the PV array current, but decreases the PV array voltage. Therefore, the duty ratio control input is

$$d(t) = -k_3 \int \dot{p}\dot{v}\,dt \tag{9}$$

or

$$d(t) = k_3 \int \dot{p}\dot{i}\,dt \tag{10}$$

where k_3 is a positive constant. Controlling the duty ratio in this fashion assures that the MPP will be continuously tracked, making RCC a true MPP tracker.

The derivatives in (9) and (10) are usually undesirable, but [64] shows that ac-coupled measurements of the PV array current and voltage can be used instead since they contain the necessary phase information. The derivatives can also be approximated by high-pass filters with cutoff frequency higher than the ripple frequency. A different and easy way of obtaining the current derivative in (10) is to sense the inductor voltage, which is proportional to the current derivative. The nonidealities in the inductor (core loss, resistance) have a small effect since the time constant of the inductor is much larger than the switching period in a practical converter.

Our present undocumented work has shown that (10) can fail due to the phase shift brought about by the intrinsic capacitance of the PV array at high switching frequencies. However, correlating power and voltage as in (9) is barely affected by the intrinsic capacitance.

Simple and inexpensive analog circuits can be used to implement RCC. An example is given in [64]. Experiments were performed to show that RCC accurately and quickly tracks the MPP, even under varying irradiance levels. The time taken to converge to the MPP is limited by the switching frequency of the power converter and the gain of the RCC circuit. Another advantage of RCC is that it does not require any prior information about the PV array characteristics, making its adaptation to different PV systems straightforward.

There are other papers in the literature that use MPPT methods that resemble RCC. For example, [65] integrates the product of the signs of the time derivatives of power and of duty ratio. However, unlike RCC, which uses inherent ripple present in current and voltage, [65] disturbs the duty ratio to generate a disturbance in power. In [66] and [67], a hysteresis-based version of RCC is used. A low frequency dithering signal is used to disturb the power in [68]. In [68], a 90° phase shift in the current (or voltage) with respect to power at the MPP is discussed, just like in RCC. The difference in [68] is that the injection is an extra, low-frequency signal and not an inherent converter ripple.

H. Current Sweep

The current sweep [69] method uses a sweep waveform for the PV array current such that the I–V characteristic of the PV array is obtained and updated at fixed time intervals. The V_{MPP} can then be computed from the characteristic curve at the same intervals.

The function chosen for the sweep waveform is directly proportional to its derivative as in

$$f(t) = k_4 \frac{df(t)}{dt} \tag{11}$$

where k_4 is a proportionality constant. The PV array power is thus given by
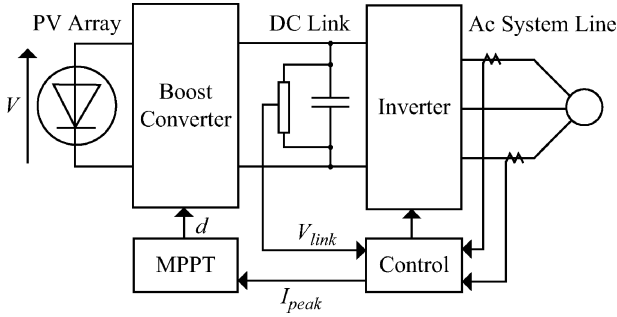
$$p(t) = v(t)\,i(t) = v(t)\,f(t). \tag{12}$$

Fig. 7. Topology for dc-link capacitor droop control as shown in [71].

At the MPP

$$\frac{dp(t)}{dt} = v(t)\frac{df(t)}{dt} + f(t)\frac{dv(t)}{dt} = 0. \tag{13}$$

Substituting (11) in (13) gives

$$\frac{dp(t)}{dt} = \left[v(t) + k_4\frac{dv(t)}{dt}\right]\frac{df(t)}{dt} = 0. \tag{14}$$

The differential equation in (11) has the following solution

$$f(t) = C\exp\left[t/k_4\right]. \tag{15}$$

C is chosen to be equal to the maximum PV array current $I_{\max}$ and k_4 to be negative, resulting in a decreasing exponential function with time constant $\tau = -k_4$. Equation (15) leads to

$$f(t) = I_{\max}\exp\left[-t/\tau\right]. \tag{16}$$

The current in (16) can be easily obtained by using some current discharging through a capacitor. Since the derivative of (16) is nonzero, (14) can be divided throughout by $df(t)/dt$ and, with $f(t) = i(t)$, (14) simplifies to

$$\frac{dp(t)}{di(t)} = v(t) + k_4\frac{dv(t)}{dt} = 0. \tag{17}$$

Once V_{MPP} is computed after the current sweep, (17) can be used to double check whether the MPP has been reached. In [69], the current sweep method is implemented through analog computation. The current sweep takes about 50 ms, implying some loss of available power. In [69], it is pointed out that this MPPT technique is only feasible if the power consumption of the tracking unit is lower than the increase in power that it can bring to the entire PV system.

I. DC-Link Capacitor Droop Control

DC-link capacitor droop control [70], [71] is an MPPT technique that is specifically designed to work with a PV system that is connected in parallel with an ac system line as shown in Fig. 7.

The duty ratio of an ideal boost converter is given by

$$d = 1 - \frac{V}{V_{link}} \tag{18}$$

where V is the voltage across the PV array and V_{link} is the voltage across the dc link. If V_{link} is kept constant, increasing
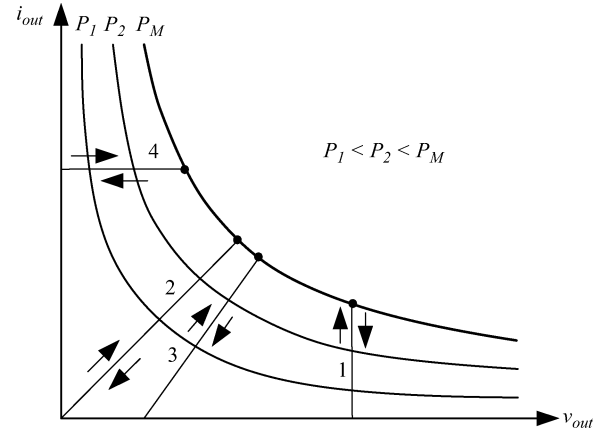

Fig. 8. Different load types. 1: voltage source, 2: resistive, 3: resistive and voltage source, 4: current source, as shown in [78].

the current going in the inverter increases the power coming out of the boost converter and consequently increases the power coming out of the PV array. While the current is increasing, the voltage V_{link} can be kept constant as long as the power required by the inverter does not exceed the maximum power available from the PV array. If that is not the case, V_{link} starts drooping. Right before that point, the current control command I_{peak} of the inverter is at its maximum and the PV array operates at the MPP. The ac system line current is fed back to prevent V_{link} from drooping and d is optimized to bring I_{peak} to its maximum, thus achieving MPPT.

DC-link capacitor droop control does not require the computation of the PV array power, but according to [71], its response deteriorates when compared to a method that detects the power directly; this is because its response directly depends on the response of the dc-voltage control loop of the inverter. This control scheme can be easily implemented with analog operational amplifiers and decision-making logic units.

J. Load Current or Load Voltage Maximization

The purpose of MPPT techniques is to maximize the power coming out of a PV array. When the PV array is connected to a power converter, maximizing the PV array power also maximizes the output power at the load of the converter. Conversely, maximizing the output power of the converter should maximize the PV array power [72]–[78], assuming a lossless converter.

In [78], it is pointed out that most loads can be of voltage-source type, current-source type, resistive type, or a combination of these, as shown in Fig. 8. From this figure, it is clear that for a voltage-source type load, the load current i_{out} should be maximized to reach the maximum output power P_M. For a current-source type load, the load voltage v_{out} should be maximized. For the other load types, either i_{out} or v_{out} can be used. This is also true for nonlinear load types as long as they do not exhibit negative impedance characteristics [78]. Therefore, for almost all loads of interest, it is adequate to maximize either the load current or the load voltage to maximize the load power. Consequently, only one sensor is needed.

In most PV systems, a battery is used as the main load or as a backup [73]–[77]. Since a battery can be thought of as a voltage-source type load, the load current can be used as the control variable. In [73], [74], and [76], positive feedback is used to control the power converter such that the load current is maximized and the PV array operates close to the MPP. Operation exactly at the MPP is almost never achieved because this MPPT method is based on the assumption that the power converter is lossless.

K. dP/dV or dP/dI Feedback Control

With DSP and microcontroller being able to handle complex computations, an obvious way of performing MPPT is to compute the slope (dP/dV or dP/dI) of the PV power curve (Fig. 2) and feed it back to the power converter with some control to drive it to zero. This is exactly what is done in [79]–[83].

The way the slope is computed differs from paper to paper. In [79], dP/dV is computed and its sign is stored for the past few cycles. Based on these signs, the duty ratio of the power converter is either incremented or decremented to reach the MPP. A dynamic step size is used to improve the transient response of the system. In [80], a linearization-based method is used to compute dP/dV. In [81]–[83], sampling and data conversion are used with subsequent digital division of power and voltage to approximate dP/dV. In [82], dP/dI is then integrated together with an adaptive gain to improve the transient response. In [83], the PV array voltage is periodically incremented or decremented and $\Delta P/\Delta V$ is compared to a marginal error until the MPP is reached. Convergence to the MPP was shown to occur in tens of milliseconds in [81].

L. Other MPPT Techniques

Other MPPT techniques include array reconfiguration [84], whereby PV arrays are arranged in different series and parallel combinations such that the resulting MPPs meet specific load requirements. This method is time consuming and tracking MPP in real time is not obvious.

In [85], a linear current control is used based on the fact that a linear relationship exists between I_{MPP} and the level of irradiance. The current I_{MPP} is thus found by sensing the irradiance level and a PI controller is used such that the PV array current follows I_{MPP}.

In [86], I_{MPP} and V_{MPP} are computed from equations involving temperature and irradiance levels, which are not usually easy to measure. Once I_{MPP} or V_{MPP} is obtained, feedback control is used to force the PV array operate at the MPP.

A state-based MPPT is introduced in [87], whereby the system is represented by a state space model, and a nonlinear time-varying dynamic feedback controller is used to track the MPP. Simulations confirm that this technique is robust and insensitive to changes in system parameters and that MPPT is achieved even with changing atmospheric conditions and in the presence of multiple local maxima caused by partially shaded PV array or damaged cells. However, no experimental verification is given.

Unlike common topologies that consist of two power stages (usually a dc–dc converter followed by an inverter), a single-stage inverter that performs both MPPT and output current regulation for utility grid distribution is introduced in [88]. Based on the voltage of the PV array, one-cycle control (OCC) is used to adjust the output current of the single-stage inverter such that MPPT is attained. The control circuit consists of discrete digital components but it can also use an inexpensive DSP. Operation is shown to be close to the MPP throughout a day-time period. The slight discrepancy is due to the inability of the controller to account for temperature variation.

The best fixed voltage (BFV) algorithm is introduced in [89]. Statistical data is collected about irradiance and temperature levels over a period of one year and the BFV representative of the MPP is found. The control sets either the operating point of the PV array to the BFV or the output voltage to the nominal load voltage. Operation is therefore never exactly at the MPP and different data has to be collected for different geographical regions.

The PV array characteristic equation, which needs to be solved iteratively for the MPP, is manipulated to find an approximate symbolic solution for the MPP in [90]. This method, called linear reoriented coordinates method (LRCM), requires the measurement of V_{OC} and I_{SC} to find the solution. Other constants representing the PV array characteristic curve are also needed. The maximum error in using LRCM to approximate the MPP was found to be 0.3%, but this was based only on simulation results.

In [91], a slide control method with a buck-boost converter is used to achieve MPPT. The switching function u of the converter is based on the fact that $dP/dV > 0$ on the left of the MPP and $dP/dV < 0$ on the right; u is expressed as

$$\begin{cases} u = 0 & S \geq 0 \\ u = 1 & S < 0 \end{cases} \tag{19}$$

where $u = 0$ means the switch is open and $u = 1$ the switch close and S is given by

$$S = \frac{dP}{dV} = I + V\frac{dI}{dV}. \tag{20}$$

This control was implemented using a microcontroller that senses the PV array voltage and current. Simulation and experimental results showed that operation converges to the MPP in several tens of milliseconds.

IV. DISCUSSION

With so many MPPT techniques available to PV system users, it might not be obvious for the latter to choose which one better suits their application needs. The main aspects of the MPPT techniques to be taken into consideration are highlighted in the following subsections.

A. Implementation

The ease of implementation is an important factor in deciding which MPPT technique to use. However, this greatly depends on the end-users' knowledge. Some might be more familiar with analog circuitry, in which case, fractional I_{SC} or V_{OC}, RCC, and load current or voltage maximization are good options. Others might be willing to work with digital circuitry, even if that

TABLE III
MAJOR CHARACTERISTICS OF MPPT TECHNIQUES

MPPT Technique	PV Array Dependent?	True MPPT?	Analog or Digital?	Periodic Tuning?	Convergence Speed	Implementation Complexity	Sensed Parameters
Hill-climbing/P&O	No	Yes	Both	No	Varies	Low	Voltage, Current
IncCond	No	Yes	Digital	No	Varies	Medium	Voltage, Current
Fractional V_{OC}	Yes	No	Both	Yes	Medium	Low	Voltage
Fractional I_{SC}	Yes	No	Both	Yes	Medium	Medium	Current
Fuzzy Logic Control	Yes	Yes	Digital	Yes	Fast	High	Varies
Neural Network	Yes	Yes	Digital	Yes	Fast	High	Varies
RCC	No	Yes	Analog	No	Fast	Low	Voltage, Current
Current Sweep	Yes	Yes	Digital	Yes	Slow	High	Voltage, Current
DC Link Capacitor Droop Control	No	No	Both	No	Medium	Low	Voltage
Load I or V Maximization	No	No	Analog	No	Fast	Low	Voltage, Current
dP/dV or dP/dI Feedback Control	No	Yes	Digital	No	Fast	Medium	Voltage, Current
Array Reconfiguration	Yes	No	Digital	Yes	Slow	High	Voltage, Current
Linear Current Control	Yes	No	Digital	Yes	Fast	Medium	Irradiance
I_{MPP} & V_{MPP} Computation	Yes	Yes	Digital	Yes	N/A	Medium	Irradiance, Temperature
State-based MPPT	Yes	Yes	Both	Yes	Fast	High	Voltage, Current
OCC MPPT	Yes	No	Both	Yes	Fast	Medium	Current
BFV	Yes	No	Both	Yes	N/A	Low	None
LRCM	Yes	No	Digital	No	N/A	High	Voltage, Current
Slide Control	No	Yes	Digital	No	Fast	Medium	Voltage, Current

may require the use of software and programming. Then, their selection should include hill climbing/P&O, IncCond, fuzzy logic control, neural network, and dP/dV or dP/dI feedback control. Furthermore, a few of the MPPT techniques only apply to specific topologies. For example, the dc-link capacitor droop control works with the system shown in Fig. 7 and the OCC MPPT works with a single-stage inverter.

B. Sensors

The number of sensors required to implement MPPT also affects the decision process. Most of the time, it is easier and more reliable to measure voltage than current. Moreover, current sensors are usually expensive and bulky. This might be inconvenient in systems that consist of several PV arrays with separate MPP trackers. In such cases, it might be wise to use MPPT methods that require only one sensor or that can estimate the current from the voltage as in [25]. It is also uncommon to find sensors that measure irradiance levels, as needed in the linear current control and the I_{MPP} and V_{MPP} computation methods.

C. Multiple Local Maxima

The occurrence of multiple local maxima due to partial shading of the PV array(s) can be a real hindrance to the proper functioning of an MPP tracker. Considerable power loss can be incurred if a local maximum is tracked instead of the real MPP. As mentioned previously, the current sweep and the state-based methods should track the true MPP even in the presence of multiple local maxima. However, the other methods require

an additional initial stage to bypass the unwanted local maxima and bring operation to close the real MPP; such examples are given in [31] and [35].

D. Costs

It is hard to mention the monetary costs of every single MPPT technique unless it is built and implemented. This is unfortunately out of the scope of this paper. However, a good costs comparison can be made by knowing whether the technique is analog or digital, whether it requires software and programming, and the number of sensors. Analog implementation is generally cheaper than digital, which normally involves a microcontroller that needs to be programmed. Eliminating current sensors considerably drops the costs.

E. Applications

Different MPPT techniques discussed earlier will suit different applications. For example, in space satellites and orbital stations that involve large amount of money, the costs and complexity of the MPP tracker are not as important as its performance and reliability. The tracker should be able to continuously track the true MPP in minimum amount of time and should not require periodic tuning. In this case, hill climbing/P&O, IncCond, and RCC are appropriate. Solar vehicles would mostly require fast convergence to the MPP. Fuzzy logic control, neural network, and RCC are good options in this case. Since the load in solar vehicles consists mainly of batteries, load current or voltage maximization should also be considered. The goal when using PV arrays in residential areas is to minimize the payback time

and to do so, it is essential to constantly and quickly track the MPP. Since partial shading (from trees and other buildings) can be an issue, the MPPT should be capable of bypassing multiple local maxima. Therefore, the two-stage InCond [31], [35] and the current sweep methods are suitable. Since a residential system might also include an inverter, the OCC MPPT can also be used. PV systems used for street lighting only consist in charging up batteries during the day. They do not necessarily need tight constraints; easy and cheap implementation might be more important, making fractional V_{OC} or I_{SC} viable.

For all other applications not mentioned here, we put together Table III, containing the major characteristics of all the MPPT techniques. Table III should help in choosing an appropriate MPPT method.

V. CONCLUSION

Several MPPT techniques taken from the literature are discussed and analyzed herein, with their pros and cons. It is shown that there are several other MPPT techniques than those commonly included in literature reviews. The concluding discussion and table should serve as a useful guide in choosing the right MPPT method for specific PV systems.

REFERENCES

[1] L. L. Buciarelli, B. L. Grossman, E. F. Lyon, and N. E. Rasmussen, "The energy balance associated with the use of a MPPT in a 100 kW peak power system," in *IEEE Photovoltaic Spec. Conf.*, 1980, pp. 523–527.

[2] J. D. van Wyk and J. H. R. Enslin, "A study of wind power converter with microprocessor based power control utilizing an oversynchronous electronic scherbius cascade," in *Proc. IEEE Int. Power Electron. Conf.*, 1983, pp. 766–777.

[3] W. J. A. Teulings, J. C. Marpinard, A. Capel, and D. O'Sullivan, "A new maximum power point tracking system," in *Proc. 24th Annu. IEEE Power Electron. Spec. Conf.*, 1993, pp. 833–838.

[4] Y. Kim, H. Jo, and D. Kim, "A new peak power tracker for cost-effective photovoltaic power system," in *Proc. 31st Intersociety Energy Convers. Eng. Conf.*, 1996, pp. 1673–1678.

[5] O. Hashimoto, T. Shimizu, and G. Kimura, "A novel high performance utility interactive photovoltaic inverter system," in *Conf. Record 2000 IEEE Ind. Applicat. Conf.*, 2000, pp. 2255–2260.

[6] E. Koutroulis, K. Kalaitzakis, and N. C. Voulgaris, "Development of a microcontroller-based, photovoltaic maximum power point tracking control system," *IEEE Trans. Power Electron.*, vol. 16, no. 21, pp. 46–54, Jan. 2001.

[7] M. Veerachary, T. Senjyu, and K. Uezato, "Maximum power point tracking control of IDB converter supplied PV system," in *IEE Proc. Elect. Power Applicat.*, 2001, pp. 494–502.

[8] W. Xiao and W. G. Dunford, "A modified adaptive hill climbing MPPT method for photovoltaic power systems," in *Proc. 35th Annu. IEEE Power Electron. Spec. Conf.*, 2004, pp. 1957–1963.

[9] O. Wasynczuk, "Dynamic behavior of a class of photovoltaic power systems," *IEEE Trans. Power App. Syst.*, vol. 102, no. 9, pp. 3031–3037, Sep. 1983.

[10] C. Hua and J. R. Lin, "DSP-based controller application in battery storage of photovoltaic system," in *Proc. IEEE IECON 22nd Int. Conf. Ind. Electron., Contr. Instrum.*, 1996, pp. 1705–1710.

[11] M. A. Slonim and L. M. Rahovich, "Maximum power point regulator for 4 kW solar cell array connected through invertor to the AC grid," in *Proc. 31st Intersociety Energy Conver. Eng. Conf.*, 1996, pp. 1669–1672.

[12] A. Al-Amoudi and L. Zhang, "Optimal control of a grid-connected PV system for maximum power point tracking and unity power factor," in *Proc. Seventh Int. Conf. Power Electron. Variable Speed Drives*, 1998, pp. 80–85.

[13] N. Kasa, T. Iida, and H. Iwamoto, "Maximum power point tracking with capacitor identifier for photovoltaic power system," in *Proc. Eighth Int. Conf. Power Electron. Variable Speed Drives*, 2000, pp. 130–135.

[14] L. Zhang, A. Al-Amoudi, and Y. Bai, "Real-time maximum power point tracking for grid-connected photovoltaic systems," in *Proc. Eighth Int. Conf. Power Electronics Variable Speed Drives*, 2000, pp. 124–129.

[15] C.-C. Hua and J.-R. Lin, "Fully digital control of distributed photovoltaic power systems," in *Proc. IEEE Int. Symp. Ind. Electron.*, 2001, pp. 1–6.

[16] M.-L. Chiang, C.-C. Hua, and J.-R. Lin, "Direct power control for distributed PV power system," in *Proc. Power Convers. Conf.*, 2002, pp. 311–315.

[17] K. Chomsuwan, P. Prisuwanna, and V. Monyakul, "Photovoltaic grid-connected inverter using two-switch buck-boost converter," in *Conf. Record Twenty-Ninth IEEE Photovoltaic Spec. Conf.*, 2002, pp. 1527–1530.

[18] Y.-T. Hsiao and C.-H. Chen, "Maximum power tracking for photovoltaic power system," in *Conf. Record 37th IAS Annu. Meeting Ind. Appl. Conf.*, 2002, pp. 1035–1040.

[19] Y. Jung, G. Yu, J. Choi, and J. Choi, "High-frequency DC link inverter for grid-connected photovoltaic system," in *Conf. Record Twenty-Ninth IEEE Photovoltaic Spec. Conf.*, 2002, pp. 1410–1413.

[20] S. Jain and V. Agarwal, "A new algorithm for rapid tracking of approximate maximum power point in photovoltaic systems," *IEEE Power Electron. Lett.*, vol. 2, no. 1, pp. 16–19, Mar. 2004.

[21] T. Tafticht and K. Agbossou, "Development of a MPPT method for photovoltaic systems," in *Canadian Conf. Elect. Comput. Eng.*, 2004, pp. 1123–1126.

[22] N. Femia, G. Petrone, G. Spagnuolo, and M. Vitelli, "Optimization of perturb and observe maximum power point tracking method," *IEEE Trans. Power Electron.*, vol. 20, no. 4, pp. 963–973, Jul. 2005.

[23] P. J. Wolfs and L. Tang, "A single cell maximum power point tracking converter without a current sensor for high performance vehicle solar arrays," in *Proc. 36th Annu. IEEE Power Electron. Spec. Conf.*, 2005, pp. 165–171.

[24] N. S. D'Souza, L. A. C. Lopes, and X. Liu, "An intelligent maximum power point tracker using peak current control," in *Proc. 36th Annu. IEEE Power Electron. Spec. Conf.*, 2005, pp. 172–177.

[25] N. Kasa, T. Iida, and L. Chen, "Flyback inverter controlled by sensorless current MPPT for photovoltaic power system," *IEEE Trans. Ind. Electron.*, vol. 52, no. 4, pp. 1145–1152, Aug. 2005.

[26] A. F. Boehringer, "Self-adapting dc converter for solar spacecraft power supply," *IEEE Trans. Aerosp. Electron. Syst.*, vol. AES-4, no. 1, pp. 102–111, Jan. 1968.

[27] E. N. Costogue and S. Lindena, "Comparison of candidate solar array maximum power utilization approaches," in *Intersociety Energy Conversion Eng. Conf.*, 1976, pp. 1449–1456.

[28] J. Harada and G. Zhao, "Controlled power-interface between solar cells and ac sources," in *IEEE Telecommun. Power Conf.*, 1989, pp. 22.1/1–22.1/7.

[29] K. H. Hussein and I. Mota, "Maximum photovoltaic power tracking: An algorithm for rapidly changing atmospheric conditions," in *IEE Proc. Generation Transmiss. Distrib.*, 1995, pp. 59–64.

[30] A. Brambilla, M. Gambarara, A. Garutti, and F. Ronchi, "New approach to photovoltaic arrays maximum power point tracking," in *Proc. 30th Annu. IEEE Power Electron. Spec. Conf.*, 1999, pp. 632–637.

[31] K. Irisawa, T. Saito, I. Takano, and Y. Sawada, "Maximum power point tracking control of photovoltaic generation system under non-uniform insolation by means of monitoring cells," in *Conf. Record Twenty-Eighth IEEE Photovoltaic Spec. Conf.*, 2000, pp. 1707–1710.

[32] T.-Y. Kim, H.-G. Ahn, S. K. Park, and Y.-K. Lee, "A novel maximum power point tracking control for photovoltaic power system under rapidly changing solar radiation," in *IEEE Int. Symp. Ind. Electron.*, 2001, pp. 1011–1014.

[33] Y.-C. Kuo, T.-J. Liang, and J.-F. Chen, "Novel maximum-power-point-tracking controller for photovoltaic energy conversion system," *IEEE Trans. Ind. Electron.*, vol. 48, no. 3, pp. 594–601, Jun. 2001.

[34] G. J. Yu, Y. S. Jung, J. Y. Choi, I. Choy, J. H. Song, and G. S. Kim, "A novel two-mode MPPT control algorithm based on comparative study of existing algorithms," in *Conf. Record Twenty-Ninth IEEE Photovoltaic Spec. Conf.*, 2002, pp. 1531–1534.

[35] K. Kobayashi, I. Takano, and Y. Sawada, "A study on a two stage maximum power point tracking control of a photovoltaic system under partially shaded insolation conditions," in *IEEE Power Eng. Soc. Gen. Meet.*, 2003, pp. 2612–2617.

[36] W. Wu, N. Pongratananukul, W. Qiu, K. Rustom, T. Kasparis, and I. Batarseh, "DSP-based multiple peak power tracking for expandable power system," in *Eighteenth Annu. IEEE Appl. Power Electron. Conf. Expo.*, 2003, pp. 525–530.

[37] H. Koizumi and K. Kurokawa, "A novel maximum power point tracking method for PV module integrated converter," in *Proc. 36th Annu. IEEE Power Electron. Spec. Conf.*, 2005, pp. 2081–2086.

[38] J. J. Schoeman and J. D. van Wyk, "A simplified maximal power controller for terrestrial photovoltaic panel arrays," in *Proc. 13th Annu. IEEE Power Electron. Spec. Conf.*, 1982, pp. 361–367.

[39] M. Buresch, *Photovoltaic Energy Systems*. New York: McGraw Hill, 1983.

[40] G. W. Hart, H. M. Branz, and C. H. Cox, "Experimental tests of open-loop maximum-power-point tracking techniques," *Solar Cells*, vol. 13, pp. 185–195, 1984.

[41] D. J. Patterson, "Electrical system design for a solar powered vehicle," in *Proc. 21st Annu. IEEE Power Electron. Spec. Conf.*, 1990, pp. 618–622.

[42] M. A. S. Masoum, H. Dehbonei, and E. F. Fuchs, "Theoretical and experimental analyses of photovoltaic systems with voltage and current-based maximum power-point tracking," *IEEE Trans. Energy Convers.*, vol. 17, no. 4, pp. 514–522, Dec. 2002.

[43] H.-J. Noh, D.-Y. Lee, and D.-S. Hyun, "An improved MPPT converter with current compensation method for small scaled PV-applications," in *Proc. 28th Annu. Conf. Ind. Electron. Soc.*, 2002, pp. 1113–1118.

[44] K. Kobayashi, H. Matsuo, and Y. Sekine, "A novel optimum operating point tracker of the solar cell power supply system," in *Proc. 35th Annu. IEEE Power Electron. Spec. Conf.*, 2004, pp. 2147–2151.

[45] B. Bekker and H. J. Beukes, "Finding an optimal PV panel maximum power point tracking method," in *Proc. 7th AFRICON Conf. Africa*, 2004, pp. 1125–1129.

[46] T. Noguchi, S. Togashi, and R. Nakamoto, "Short-current pulse based adaptive maximum-power-point tracking for photovoltaic power generation system," in *Proc. 2000 IEEE Int. Symp. Ind. Electron.*, 2000, pp. 157–162.

[47] N. Mutoh, T. Matuo, K. Okada, and M. Sakai, "Prediction-data-based maximum-power-point-tracking method for photovoltaic power generation systems," in *Proc. 33rd Annu. IEEE Power Electron. Spec. Conf.*, 2002, pp. 1489–1494.

[48] S. Yuvarajan and S. Xu, "Photo-voltaic power converter with a simple maximum-power-point-tracker," in *Proc. 2003 Int. Symp. Circuits Syst.*, 2003, pp. III-399–III-402.

[49] R. M. Hilloowala and A. M. Sharaf, "A rule-based fuzzy logic controller for a PWM inverter in photo-voltaic energy conversion scheme," in *Proc. IEEE Ind. Appl. Soc. Annu. Meet.*, 1992, pp. 762–769.

[50] C.-Y. Won, D.-H. Kim, S.-C. Kim, W.-S. Kim, and H.-S. Kim, "A new maximum power point tracker of photovoltaic arrays using fuzzy controller," in *Proc. 25th Annu. IEEE Power Electron. Spec. Conf.*, 1994, pp. 396–403.

[51] T. Senjyu and K. Uezato, "Maximum power point tracker using fuzzy control for photovoltaic arrays," in *Proc. IEEE Int. Conf. Ind. Technol.*, 1994, pp. 143–147.

[52] G.-J. Yu, M.-W. Jung, J. Song, I.-S. Cha, and I.-H. Hwang, "Maximum power point tracking with temperature compensation of photovoltaic for air conditioning system with fuzzy controller," in *Proc. IEEE Photovoltaic Spec. Conf.*, 1996, pp. 1429–1432.

[53] M. G. Simoes, N. N. Franceschetti, and M. Friedhofer, "A fuzzy logic based photovoltaic peak power tracking control," in *Proc. IEEE Int. Symp. Ind. Electron.*, 1998, pp. 300–305.

[54] A. M. A. Mahmoud, H. M. Mashaly, S. A. Kandil, H. El Khashab, and M. N. F. Nashed, "Fuzzy logic implementation for photovoltaic maximum power tracking," in *Proc. 9th IEEE Int. Workshop Robot Human Interactive Commun.*, 2000, pp. 155–160.

[55] N. Patcharaprakiti and S. Premrudeepreechacharn, "Maximum power point tracking using adaptive fuzzy logic control for grid-connected photovoltaic system," in *IEEE Power Eng. Soc. Winter Meet.*, 2002, pp. 372–377.

[56] B. M. Wilamowski and X. Li, "Fuzzy system based maximum power point tracking for PV system," in *Proc. 28th Annu. Conf. IEEE Ind. Electron. Soc.*, 2002, pp. 3280–3284.

[57] M. Veerachary, T. Senjyu, and K. Uezato, "Neural-network-based maximum-power-point tracking of coupled-inductor interleaved-boost-converter-supplied PV system using fuzzy controller," *IEEE Trans. Ind. Electron.*, vol. 50, no. 4, pp. 749–758, Aug. 2003.

[58] N. Khaehintung, K. Pramotung, B. Tuvirat, and P. Sirisuk, "RISC-microcontroller built-in fuzzy logic controller of maximum power point tracking for solar-powered light-flasher applications," in *Proc. 30th Annu. Conf. IEEE Ind. Electron. Soc.*, 2004, pp. 2673–2678.

[59] T. Hiyama, S. Kouzuma, and T. Imakubo, "Identification of optimal operating point of PV modules using neural network for real time maximum power tracking control," *IEEE Trans. Energy Convers.*, vol. 10, no. 2, pp. 360–367, Jun. 1995.

[60] K. Ro and S. Rahman, "Two-loop controller for maximizing performance of a grid-connected photovoltaic-fuel cell hybrid power plant," *IEEE Trans. Energy Convers.*, vol. 13, no. 3, pp. 276–281, Sep. 1998.

[61] A. Hussein, Y. Hirasawa, J. Hu, and J. Murata, "The dynamic performance of photovoltaic supplied dc motor fed from DC–DC converter and controlled by neural networks," in *Proc. Int. Joint Conf. Neural Netw.*, 2002, pp. 607–612.

[62] X. Sun, W. Wu, X. Li, and Q. Zhao, "A research on photovoltaic energy controlling system with maximum power point tracking," in *Proc. Power Convers. Conf.*, 2002, pp. 822–826.

[63] L. Zhang, Y. Bai, and A. Al-Amoudi, "GA-RBF neural network based maximum power point tracking for grid-connected photovoltaic systems," in *Proc. Int. Conf. Power Electron., Machines and Drives*, 2002, pp. 18–23.

[64] P. Midya, P. T. Krein, R. J. Turnbull, R. Reppa, and J. Kimball, "Dynamic maximum power point tracker for photovoltaic applications," in *Proc. 27th Annu. IEEE Power Electron. Spec. Conf.*, 1996, pp. 1710–1716.

[65] V. Arcidiacono, S. Corsi, and L. Lambri, "Maximum power point tracker for photovoltaic power plants," in *Proc. IEEE Photovoltaic Spec. Conf.*, 1982, pp. 507–512.

[66] Y. H. Lim and D. C. Hamill, "Simple maximum power point tracker for photovoltaic arrays," *Electron. Lett.*, vol. 36, pp. 997–999, May 2000.

[67] ——, "Synthesis, simulation and experimental verification of a maximum power point tracker from nonlinear dynamics," in *Proc. 32nd Annu. IEEE Power Electron. Spec. Conf.*, 2001, pp. 199–204.

[68] L. Stamenic, M. Greig, E. Smiley, and R. Stojanovic, "Maximum power point tracking for building integrated photovoltaic ventilation systems," in *Proc. IEEE Photovoltaic Spec. Conf.*, 2000, pp. 1517–1520.

[69] M. Bodur and M. Ermis, "Maximum power point tracking for low power photovoltaic solar panels," in *Proc. 7th Mediterranean Electrotechnical Conf.*, 1994, pp. 758–761.

[70] M. Matsui, T. Kitano, D.-h. Xu, and Z.-q. Yang, "A new maximum photovoltaic power tracking control scheme based on power equilibrium at DC link," in *Conf. Record 1999 IEEE Ind. Appl. Conf.*, 1999, pp. 804–809.

[71] T. Kitano, M. Matsui, and D.-h. Xu, "Power sensor-less MPPT control scheme utilizing power balance at DC link-system design to ensure stability and response," in *Proc. 27th Annu. Conf. IEEE Ind. Electron. Soc.*, 2001, pp. 1309–1314.

[72] E. E. Landsman, *Maximum Power Point Tracker for Photovoltaic Arrays*. Boston, MA: Massachusetts Institute of Technology Lincoln Labs, 1978.

[73] J. H. R. Enslin and D. B. Snyman, "Simplified feed-forward control of the maximum power point in PV installations," in *Proc.1992 Int. Conf. Ind. Electron., Contr., Instrum., and Automat.*, 1992, pp. 548–553.

[74] H. J. Beukes and J. H. R. Enslin, "Analysis of a new compound converter as MPPT, battery regulator and bus regulator for satellite power systems," in *Proc. 24th Annu. IEEE Power Electron. Spec. Conf.*, 1993, pp. 846–852.

[75] C. R. Sullivan and M. J. Powers, "A high-efficiency maximum power point tracker for photovoltaic arrays in a solar-powered race vehicle," in *Proc. 24th Annu. IEEE Power Electron. Spec. Conf.*, 1993, pp. 574–580.

[76] A. S. Kislovski and R. Redl, "Maximum-power-tracking using positive feedback," in *Proc. 25th Annu. IEEE Power Electron. Spec. Conf.*, 1994, pp. 1065–1068.

[77] J. Arias, F. F. Linera, J. Martin-Ramos, A. M. Pernia, and J. Cambronero, "A modular PV regulator based on microcontroller with maximum power point tracking," in *Proc. IEEE Ind. Appl. Conf.*, 2004, pp. 1178–1184.

[78] D. Shmilovitz, "On the control of photovoltaic maximum power point tracker via output parameters," in *IEE Proc. Elect. Power Appl.*, 2005, pp. 239–248.

[79] R. Bhide and S. R. Bhat, "Modular power conditioning unit for photovoltaic applications," in *Proc. 23rd Annu. IEEE Power Electron. Spec. Conf.*, 1992, pp. 708–713.

[80] H. Sugimoto and H. Dong, "A new scheme for maximum photovoltaic power tracking control," in *Proc. Power Convers. Conf.*, 1997, pp. 691–696.

[81] S. J. Chiang, K. T. Chang, and C. Y. Yen, "Residential photovoltaic energy storage system," *IEEE Trans. Ind. Electron.*, vol. 45, no. 3, pp. 385–394, Jun. 1998.

[82] J. A. M. Bleijs and A. Gow, "Fast maximum power point control of current-fed DC–DC converter for photovoltaic arrays," *Electron. Lett.*, vol. 37, pp. 5–6, Jan. 2001.

[83] C.-L. Hou, J. Wu, M. Zhang, J.-M. Yang, and J.-P. Li, "Application of adaptive algorithm of solar cell battery charger," in *Proc. IEEE Int. Conf. Elect. Utility Deregulation Restruct. Power Technol.*, 2004, pp. 810–813.

[84] M. A. El-Shibini and H. H. Rakha, "Maximum power point tracking technique," in *Proc. Integrating Research, Ind. Educ. Energy Commun. Eng. Electrotechnical Conf.*, 1989, pp. 21–24.

[85] C.-T. Pan, J.-Y. Chen, C.-P. Chu, and Y.-S. Huang, "A fast maximum power point tracker for photovoltaic power systems," in *Proc. 25th Annu. Conf. IEEE Ind. Electron. Soc.*, 1999, pp. 390–393.

[86] T. Takashima, T. Tanaka, M. Amano, and Y. Ando, "Maximum output control of photovoltaic (PV) array," in *Proc. 35th Intersociety Energy Convers. Eng. Conf. Exhib.*, 2000, pp. 380–383.

[87] E. V. Solodovnik, S. Liu, and R. A. Dougal, "Power controller design for maximum power tracking in solar installations," *IEEE Trans. Power Electron.*, vol. 19, no. 5, pp. 1295–1304, Sep. 2004.

[88] Y. Chen and K. M. Smedley, "A cost-effective single-stage inverter with maximum power point tracking," *IEEE Trans. Power Electron.*, vol. 19, no. 5, pp. 1289–1294, Sep. 2004.

[89] P. C. M. de Carvalho, R. S. T. Pontes, D. S. Oliveira, Jr., D. B. Riffel, R. G. V. de Oliveira, and S. B. Mesquita, "Control method of a photovoltaic powered reverse osmosis plant without batteries based on maximum power point tracking," in *Proc. IEEE/PES Transmiss. Distrib. Conf. Expo.: Latin America*, 2004, pp. 137–142.

[90] E. I. rtiz-Rivera and F. Peng, "A novel method to estimate the maximum power for a photovoltaic inverter system," in *Proc. 35th Annu. IEEE Power Electron. Spec. Conf.*, 2004, pp. 2065–2069.

[91] M. Zhang, J. Wu, and H. Zhao, "The application of slide technology in PV maximum power point tracking system," in *Proc. Fifth World Congr. Intell. Contr. Automat.*, 2004, pp. 5591–5594.

Patrick L. Chapman (S'94–M'00–SM'05) received the B.S. and M.S. degrees from the University of Missouri-Rolla, Rolla, MO, in 1996 and 1997, respectively, and the Ph.D. degree from Purdue University, West Lafayette, IN, in 2000, all in electrical engineering.

Currently, he is a Grainger Associate and Assistant Professor in the Department of Electrical and Computer Engineering at the University of Illinois at Urbana-Champaign, Urbana, IL. He is a co-founder of SmartSpark Energy Systems, Inc. His research interests, within power electronics, include integrated design, automated modeling, hybrid energy systems, and energy harvesting.

Dr. Chapman is a Senior Member of the IEEE, an Associate Editor for IEEE TRANSACTIONS ON POWER ELECTRONICS, and a Member-at-Large for the IEEE Power Electronics Society Administrative Committee. He is the recipient of the National Science Foundation CAREER Award and the Office of Naval Research Young Investigator Award. He was named the Richard M. Bass Outstanding Young Power Electronics Engineer in 2006.
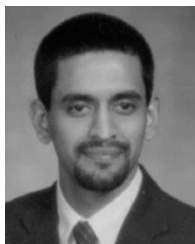
Trishan Esram (S'00) received the B.S. degree from Northeastern University, Boston, MA, in 2003, in electrical engineering, and the M.S. degree in electrical engineering from the University of Illinois at Urbana-Champaign, Urbana, IL, in 2004. Currently, he is working toward the Ph.D. degree in optimal control of power converters and alternative energy sources at the University of Illinois at Urbana-Champaign, as a Research Assistant for Prof. P. L. Chapman.